Multimodal shunt damping of monolithic bladed drums using multiple digital vibration absorbers

Jennifer Dietrich
PhD in Engineering and Technology
Space Structures and Systems Laboratory (S3L)
Email: jdietrich@uliege.be

Ghislain Raze
Postdoctoral researcher
Space Structures and Systems Laboratory (S3L)
Email: g.raze@uliege.be

Xavier Charles
Safran Aero Boosters, Herstal, Belgium

Gaëtan Kerschen
Full professor
Space Structures and Systems Laboratory (S3L)
University of Liège
Liège, Belgium-4000
Email: g.kerschen@uliege.be

Based on a digital realization of piezoelectric shunt circuits, this works presents a proof-of-concept damping approach tailored to address the complex dynamics of monolithic bladed drums (BluMs) and attenuate their vibrations. This approach comprises the simultaneous use of multiple digital vibration absorbers (DVAs) together with a mean shunt strategy, taking advantage of the fact that multiple absorbers act simultaneously on the structure and that the blade modes of BluMs appear closely-spaced. In order to target multiple groups of modes, this strategy is incorporated in a multi-staged shunt circuit. The damping concept is numerically and experimentally demonstrated on a BluM with multiple piezoelectric patches, proving its ability to achieve excellent damping performance on multiple groups of modes. This performance is shown to be relatively insensitive to the spatial distribution of the shunted patches. Based on a robustness study, it was also found that the shunts are robust to changes in the host structure which could, e.g., be due to mistuning. Owing their digital nature, DVAs are easily adjustable making them highly attractive in practical applications.

1 INTRODUCTION

The question of how to combine the desire to travel with the need to protect the environment has gained significant attention over the past decades and the importance of CO_2 reduction poses new challenges for aerospace engineers. In a mid-term perspective, the trend goes toward more lightweight rotor designs. Yet, some challenges come along with these solutions as they often exhibit low structural damping, causing large vibrations that can increase susceptibility to nonlinear behaviors, fatigue and, consequently, failure. It is thus preferable to avoid excitation of the resonance frequencies of the structure. If this is not possible, it is of utmost importance to attenuate the resonant vibrations by means of additional damping.

The structure of interest in this work is a part of a rotor stage of an aircraft engine, namely a low-pressure compressor rotor called BluM. Realized as a single piece, it consists of a drum with a multitude of blades, attached at the circumference without any interfaces. As parts of an aircraft engine, these components are exposed to two types of external forces, mechanical and aerodynamic. The former is caused by mechanical interactions (rotor/stator contact) or a rotor imbalance, while the latter follows from the airflow entering the fan and passing through the engine stages [1]. Moreover, small imperfections in the manufacturing process (the so-called mistuning effect), which disturb the cyclic symmetry of BluMs, can cause localization of vibration followed by fatigue

failures. Mitigating the vibrations of these structures can reduce the risk of such failures and becomes thus an important issue for the aerospace engineer.

There exist different damping strategies for bladed structures, among them the popular concept of mechanical friction dampers. In [2], blade root attachments were proposed as good candidates for non-monolithic bladed drums/disks. Further, to avoid disturbances of the airflow, underplatform dampers [3] or friction ring dampers [4] were used. We note that frictional damping presents two main difficulties, namely that relative displacement causes the desired energy dissipation, which means that not all modes can be addressed. In addition, the numerical prediction of their nonlinear behavior can be challenging and time consuming. Nguyen et al. proposed the use of viscoelastic materials placed between the blade root and the disk [5] that could be translated into viscoelastic coating for mono-pieces. However, this approach cannot be used at high temperatures. Another promising damping approach consists in piezoelectric shunt damping.

Piezoelectric shunt damping solutions for bladed structures with piezoelectric patches mounted on the blades were presented in e.g. [6, 7, 8]. In the context of industrial applications, however, this should be avoided in order to prevent interaction with the air flow. With an acceptable trade-off between the aerodynamic performance and the electromechanical coupling, piezoelectric patches may be placed under the blade roots inside the drum/disk as in the works of Mokrani et al. [9, 10], Zhou et al. [11] and Viguié et al. [12]. Mokrani et al. used multiple piezoelectric patches in parallel to piezoelectric shunt circuits to damp the vibrations of a BluM. While the strategy yielded a satisfying damping performance over the first group of blade modes, it could not prove robust toward mistuning [13]. In [11], Zhou et al. mimicked a nonlinear energy sink with piezoelectric shunts that was robust and efficient over a large frequency band but difficult to design. In [14], pairs of piezoelectric patches were installed under the blade roots of a bladed rail structure to damp their vibrations with PPF controllers, exploiting an active control law. Recently, a similar bladed rail structure was subject in the work of Dietrich et al. using resonant piezoelectric shunt circuits working according to a passive control law adapted to the particular and challenging dynamics of bladed structures with multiple shunt circuits [15]. The circuits were realized with digital controllers – herein called digital vibration absorbers (DVAs). This idea of a digital shunt impedance, which was first introduced by Fleming et al. in [16], allows the user to impose any desired relation between a measured voltage V_p of the piezoelectric electrode and a current $\dot{q}_p$ that is sent back to it using a digital signal processing unit. This enables the emulation of sophisticated circuit designs and the adjustment of shunt parameters in case of mistuning or other changes in the host system. In [17], through detailed numerical simulations, Raze proved the efficiency of different piezoelectric tuning strategies on a BluM. To the best of our knowledge, a digital realization of a passive piezoelectric shunt circuit has never been applied to a real cyclic bladed structure.

This work takes the developments from [15] on a next level by applying them to a BluM that was already subject to the studies of Mokrani et al. [9, 10, 13]. This structure exhibits a high modal density posing particular challenges. By using a digital realization of piezoelectric shunt circuits, we take advantage of the fact that DVAs are versatile, compact and easy to implement. Through detailed numerical and experimental studies, this work features three original contributions, namely

a) a demonstration of the vibration mitigation performance of the proposed strategy leveraging multiple shunt circuits emulated with DVAs for a BluM. This represents a substantial challenge for piezoelectric tuned vibration absorbers, which are, with only a handful of exceptions, demonstrated on simple academic structures, such as beams, trusses, plates and simple shells. The structure treated in this work features both isolated and closely-spaced resonance frequencies, and a robust tuning approach is used to address this issue. To the authors' knowledge, this work represents the first experimental validation of broadband piezoelectric shunt damping on a complex industrial structure. This performance is enabled thanks to the versatility of the digital approach used herein.
b) a study of the influence of the number of shunted patches and their spatial distribution. The performance of piezoelectric tuned vibration absorbers is contingent upon the electromechanical coupling of the piezoelectric transducer with the targeted mode, making the spatial location of the latter crucial for performance. In this work, the impact of the choice of a subset of transducers is assessed and shown to have little impact on performance.
c) a preliminary assessment of the robustness of the approach against mistuning. Since piezoelectric tuned vibration absorbers are sensitive to frequency shifts in the host structure, ensuring the robustness of the proposed approach is essential. The structure is intentionally mistuned in a random-like pattern to assess the effects of mistuning. A retuning procedure, eased by the digital approach leveraged in this work, is also demonstrated to be an effective solution.

This work is structured as follows. Section 2 presents the BluM under study, and Section 3 briefly reviews the strategy used to deal with its challenging dynamics. This strategy is first numerically assessed in Section 4. Section 5 presents the DVAs that are used to enable an experimental realization assessed in Section 6. A discussion about this proof of concept is made in Section 7, before concluding this work in Section 8.

2 THE BLUM STRUCTURE

The BluM already used in the works of Mokrani et al. [9, 10, 13] is considered in this work. The BluM is a rotor of a low-pressure compressor stage featuring 76 blades and is made of a titanium alloy. This is a monolithic part, whose drum was machined and to which the blades were friction-welded. It was provided by Safran Aero Boosters. For this reason, all sensitive data about the structure are normalized with the magnitude and frequency related to the first mode of mode family #1 in what follows.

Due to the lack of mechanical interfaces, the BluM exhibits very low damping (of the order of $0.01\,\%$ [9]), calling for damping enhancement solutions. This is what motivated Mokrani et al. [13] to target the first family of modes with analog circuits. By contrast, this work relies on a digital shunt realization with DVAs. Using DVAs, we can achieve greater tuning flexibility and eliminate the need for synthetic inductors. 28 PI-PIC255 piezoceramic patches ($40mm \times 10mm \times 200\mu m$) were fixed with conductive glue in the support drum under the blade roots. One patch was approximately covering three blades. Due to limitations of the digital controller unit (MicroLabBox from dSpace) that was available in the laboratory, only 16 out of the 28 available patches could be used simultaneously. The experimental BluM connected to the DVAs is presented in Fig. 1. Thanks to their relatively compact realization on printed circuit boards (PCBs), the DVAs could be directly installed on the drum.

The BluM was bolted to an optical breadboard, approximating clamped boundary conditions. As already remarked by Mokrani et al. [13], the structure exhibits inevitable mistuning. In particular, the 28 patches break the rotational symmetry of the bare BluM. Small magnets of $1.3\mathrm{g}$ were fixed at the tip blades of the structure as they used to excite it in previous studies [9, 10, 13], introducing another source of mistuning. Later in the experimental campaign, in the context of a robustness study, these magnets were partly removed to alter the structure and simulate random mistuning.

Bladed structures exhibit particular dynamic properties that are preserved even when the cyclic symmetry is disturbed due to e.g. mistuning. They exhibit a high number of modes with the ones related to the blade motions appearing in groups of closely-spaced frequencies. These groups are called mode families and are associated with a respective blade mode shape. A full description of the dynamic behavior of these structures can be found in [18].

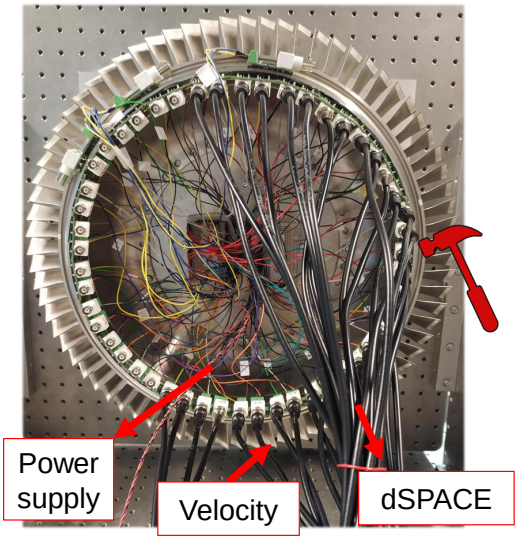

Fig. 1: Photograph of the BluM setup with DVAs. The hammer indicates the location of the excitation.

In Fig. 2, the frequency response function (FRF) of the BluM with open-circuited patches is displayed with a zoom on the first mode family that is associated with the first bending modes of the blades [9]. Details about the experimental procedure to obtain this FRF are given in Section 6. We observe that the modes indeed appear closely-spaced. Around the mode family, there appear modes in a more scattered pattern, corresponding to the modes of the drum support.

3 DAMPING STRATEGIES FOR STRUCTURES WITH HIGH MODAL DENSITIES

In this work, we use a shunt tuning strategy tailored to mitigate the vibrations of a BluM and to cope with its high modal density. Multiple DVAs are tuned in order to effectively damp the multitude of modes that appear in a mode family. The tuning strategy used in this work was already presented in [15] and experimentally demonstrated on a bladed rail, featuring mode families of five modes. This work takes this strategy proposed in that previous work to the next level by applying it to the BluM.

A conventional resonant piezoelectric shunt is constituted of a resistor and an inductor, and can be connected to a piezoelectric transducer to mitigate a specific struc-

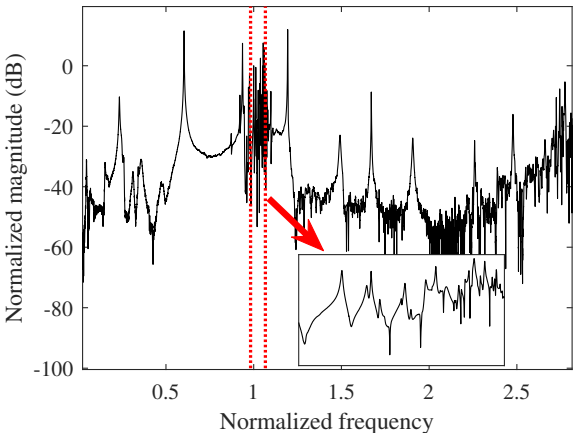

Fig. 2: Open-circuit FRF with zoom on mode family #1.

tural resonance. When the structure vibrates, a part of its mechanical energy is converted into electrical one by the transducer. The inductance is tuned to create an electrical resonance with the capacitance of the patch that matches the targeted mechanical resonance, boosting the energy dissipation in the resistor and resulting in effective damping of the mechanical resonance. Multiple mechanical resonances can be mitigated with more sophisticated circuits possessing multiple shunt branches [19, 20]. The presence of multiple branches results in multiple electrical resonances, which are matched to the target mechanical resonances to mitigate them. Alternatively, if the target modes are closely spaced in frequency, a mean shunt strategy can be used, wherein one electrical resonance frequency is placed at the average value of the mechanical resonant frequencies [9].

To target multiple modes of a BluM, the multi-staged current blocking approach leveraged by Raze et al. [21] was exploited in this work. Other circuits exist for the purpose of multimodal vibration mitigation and are rather equivalent in terms of performance [22]. Furthermore, to cope with the high modal density featured by a mode family, we incorporate in this approach the possibility to use a shunt branch to implement a mean shunt. Each circuit branch can thus be aimed to resonate with the mean frequency of a mode family, or an isolated mode, e.g. a drum mode.

Multiple transducers are used to mitigate the numerous modes of the structure. This provides a better electromechanical coupling with the targeted modes than an approach with a single transducer, improving the damping performance. The proposed approach accounts for the fact that multiple shunts simultaneously target the same resonances. Fig. 3 summarizes this approach: to each shunted patch is connected a multi-stage shunt circuit, whose branches target different frequencies or frequency ranges.

An important feature of the strategy is that it does not require a numerical model of the structure, and that all quantities required to tune the shunts can be found in the dynamic impedance of a transducer, i.e., the transfer function between the voltage V_p across the electrodes of the transducer and the current sq_p flowing through them (where s is Laplace's variable). It can be shown [15] that this relation is

$$\begin{aligned}\frac{V_p}{sq_p} &= -\frac{1}{sC_p^\varepsilon}\left[1-\sum_{k=1}^{K}\frac{\theta_{\phi,k}}{s^2+\omega_{\mathrm{oc},k}^2}\right] \\ &= -\frac{1}{sC_p^\varepsilon}\frac{\prod_{k=1}^{K}(s^2+\omega_{sc,k,p}^2)}{\prod_{k=1}^{K}(s^2+\omega_{oc,k}^2)},\end{aligned} \tag{1}$$

where C_p^ε is the capacitance of the piezoelectric transducer at constant strain, $\omega_{\mathrm{oc},k}$ is the k^{th} resonance frequency of the structure with open-circuited transducers, $\theta_{\phi,k} \geq 0$ is its associated modal amplitude (seen from the transducer), and $\omega_{sc,k,p}$ is the resonance frequency of the structure when transducer p is short-circuited (every other transducer being in open circuit). The tuning procedure only requires the resonance and antiresonance frequencies, as well as the capacitance C_p^ε, which can easily be identified from measurements of the dynamic impedance. It then tunes the parameters of the shunt circuit to provide effective multimodal damping. For reasons of brevity, only the underlying ideas of the tuning procedure are described herein and the reader is referred to [15, 17, 21] for a detailed description.

4 SUPPORTING NUMERICAL STUDY

Prior to the experimental campaign, numerical simulations were conducted on an FE model of the BluM with a modal damping of $0.01\,\%$, as is typical in these structures [9] and close to the experimental measurements. This model, already used for numerical investigations in [17], consists of linear shell elements and incorporates the piezoelectric behavior of the patches [23] to allow to couple the structure to shunt models. The degrees of freedom in the part of the drum attached to the optical breadboard were fixed to approximate the experimental boundary conditions. The full model possesses more than one million degrees of freedom, and was reduced using a Craig-Bampton approach, retaining degrees of freedom at several blade tips and at the excitation location, as well as the electrical degrees of freedom of the patches elec-

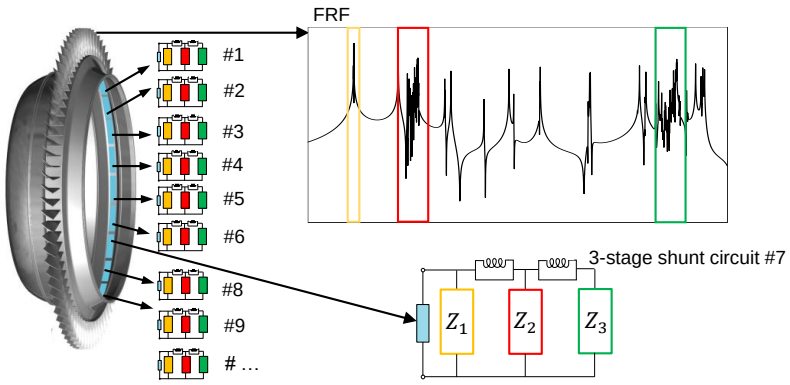

Fig. 3: Exploitation of several multi-staged shunt circuits on a BluM example. The circuits operate simultaneously, being connected to different piezoelectric patches. One stage each is tuned toward a particular frequency (range) of the host structure FRF, as indicated by the colors.

trodes, and keeping 200 component normal modes to ensure a correct representation of the first two families. The reduced-order models, comprising 420 degrees of freedom, were then coupled with shunt circuits in Matlab. Our numerical study comprises model variations with different cases of mistuning along with different configurations of the 16 patches in order to investigate if certain patch configurations outperform the others. More concretely, the goal of this study was to investigate

a) if 16 patches are sufficient to achieve a satisfying damping performance,
b) if some patch configurations outperform the damping performances of others,
c) if some patch configurations are more robust toward different cases of mistuning,
d) and to demonstrate the efficiency of the proposed damping strategies on two mode families.

To address these points, we evaluated the amplitude reduction in the frequency range of mode family #1 (between frequencies 1.00 and 1.08) achieved by mean shunts tuned toward their mean frequency and implemented in single RL shunts. The assessment of this amplitude reduction took place by comparing the average of the H_2 norm of 25 FRFs taken at different blade tip locations of the system in (i) open circuit and (ii) of the controlled system.

Firstly, addressing a), the mean amplitude reduction of the FRF of mode family #1 as a function of the number of active piezoelectric patches is shown in Fig. 4 (with no mistuning present). Here, the piezoelectric patches with the highest coupling factors (over all modes) were used. Using a small number of patches, it can be observed that the amplitude reduction increases sharply. For example,

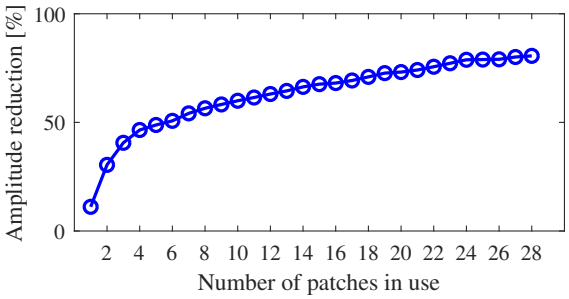

Fig. 4: Amplitude reduction for mode family #1 as a function of the number of active piezoelectric patches (case without mistuning).

with only 6 patches, the FRF amplitudes can be already reduced by approximately 50 %. The smaller increase of the curve for a higher number of patches indicates that not all patches need to be used simultaneously to achieve a satisfying damping performance on this family of modes.

To investigate b), five different patch configurations (Config. 1-5) were used to implement 16 single RL shunts tuned according to the mean shunt strategy. They are displayed in Fig. 5. The case with no mistuning present as well as three randomly chosen cases of mistuning were considered, with the shunts always being tuned optimally for each mistuned case. It was found that no particular patch configuration exhibited superior performance and that a mean amplitude reduction of more than 60 % could be achieved with all different patch configurations (40 % in the worst case scenario). A summary of these results is illustrated in Fig. 6. Here, the mean amplitude reduction of the modes belonging to mode family #1 is presented

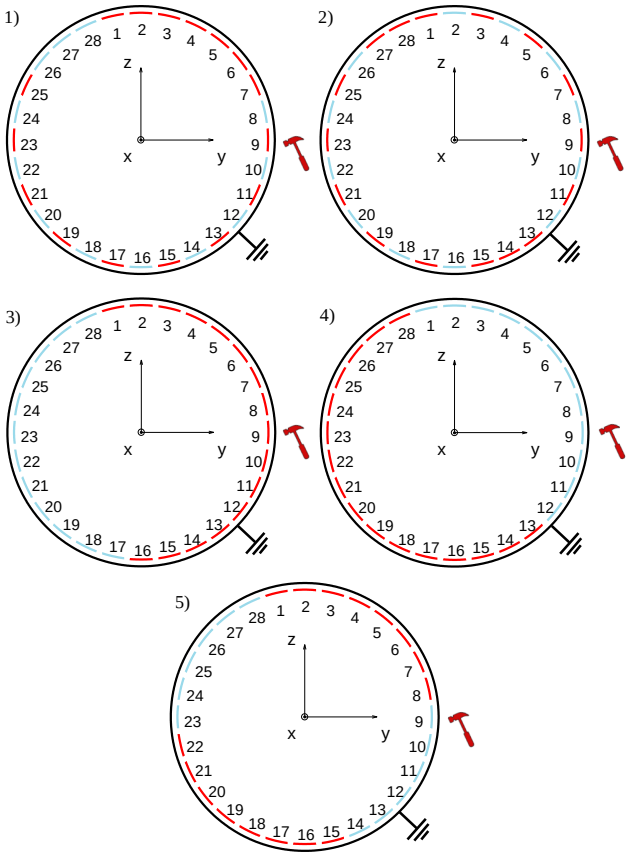

Fig. 5: Different configurations of the piezoelectric patches (where patches colored in red are shunted). The numbers 1-5 refer to the respective configuration. The hammer indicates the impact location.

for each configuration showing that all configurations not only yield excellent damping performances but were also robust towards mistuning. This shows the direct comparison between the amplitude reductions achieved by shunts tuned according to the respective case of mistuning with detuned shunts, tuned towards the case of no mistuning present (cf. Fig. 6): The reduction is either almost identical or only slightly less with the detuned shunts. Additionally, examining the coupling of the patches, it could be noted that the electromechanical coupling was best with no mistuning present.

Addressing c), the different patch configurations were then systematically used with shunts tuned to the case where no mistuning is present – unlike the previous case, no shunt retuning took place. By comparing the mean amplitude reductions under the different patch configurations it can be stated no patch configuration significantly outperforms the other ones.

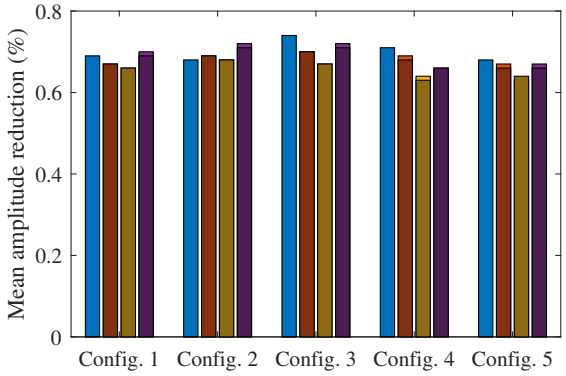

Fig. 6: Mean amplitude reduction of mode family #1 with five different patch configurations. The color of each bar stands of a different case of mistuning (where (▬) represents the case without mistuning). Faded and bright colors are related to shunts tuned toward the respective configurations without and with mistuning, respectively.

Two mode families were targeted simultaneously with one shunt circuit per patch to verify d). In order to demonstrate the effectiveness of the strategy proposed in Section 3, the multi-staged shunt circuits were applied to the numerical model. Using Config. 3 in Fig. 5, 16 two-stage shunt circuits tuned to target the mean frequencies of mode families #1 and #2 were implemented. The mobility functions from the impact force to the velocity measured at a tip blade located around patch 11 (cf. Fig. 1) for the uncontrolled and the controlled systems are displayed in Fig. 7, covering the frequency ranges of both mode families. It can be observed that the shunts yielded resonance amplitude reductions for both mode family #1 (around normalized frequency 1) and #2 (around normalized frequency 2.5) of up to 20 dB and 15 dB, respectively. In terms of H_2 norm reduction, 30.77 % and 25.23 % are obtained for mode families #1 and #2, respectively. It should be noted that this comes at the cost of a loss in damping performance due to the fact that a passive control law is used. The available control authority needs now to be distributed over two frequency ranges. Yet, reductions of the resonance amplitudes remain highly satisfactory.

Finally, we come back simultaneously to a) and d) to show why the approach is expected to provide the same type of performance on all blades. Fig. 8 presents the modal damping ratios of the targeted modes without and with control on one or two mode families. Clearly, the approaches enhance the modal damping of all targeted modes, showing that the damping performance can globally be expected on the structure.

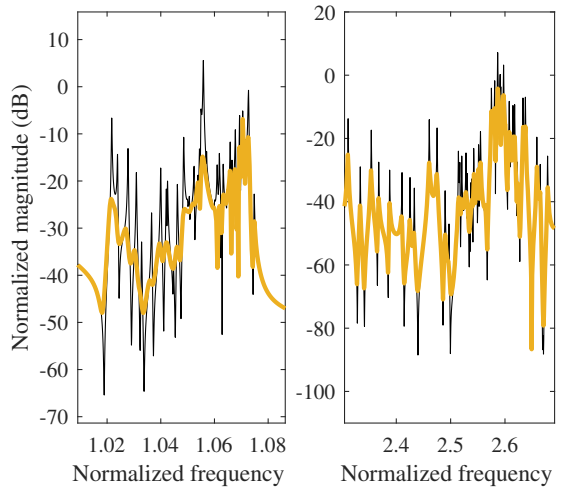

Fig. 7: FRF of a mistuned BluM with a close-up on mode families #1 and #2. The uncontrolled case (▬) is compared to a system controlled by a multi-stage shunt (▬).

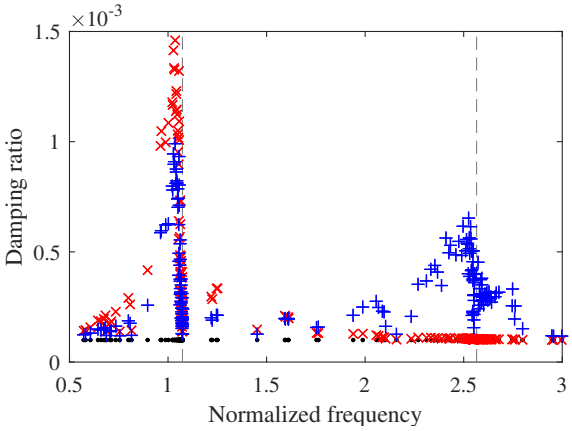

Fig. 8: Normalized resonance frequency vs. modal damping ratio: uncontrolled (•), mean shunt (×) and multi-stage shunt (+). The targeted mean frequencies are represented using (▪▪▪).

5 A DIGITAL VIBRATION ABSORBER

The proposed strategy was shown to be effective numerically but can be complex to implement experimentally. In theory, shunts can be realized with analog circuits in a fully passive way. However, the required inductances are generally much larger than what is commercially available, and synthetic inductors realized with active components need to be used instead [9]. These solutions however usually lack compactness, feature non-ideal behavior and are complicated to fine-tune.

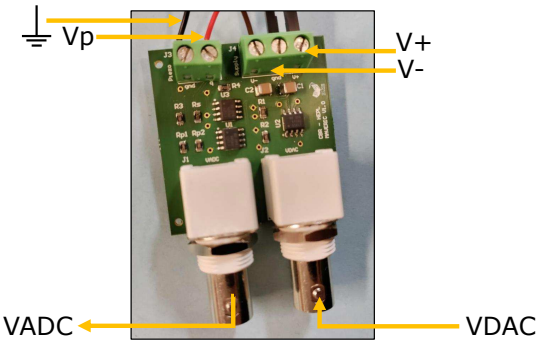

Fig. 9: Picture of a DVA used in this work.

In this work, DVAs are thus used to circumvent the aforementioned issues. The DVAs that were used to realize the piezoelectric shunts are shown in Figure 9 and consist of an analog circuit and a digital unit [16]. They are used to replicate the action of a shunt by imposing the desired current/voltage (admittance) relation of the shunt. In the implementation used herein, a sensing element measures the voltage V_p of the patch. This signal is then fed to the digital unit which emulates the patch admittance, thereby computing the current in the shunt that is to be injected in the patch $\dot{q}_p$. This is performed thanks a current source in the DVA. DVAs feature great versatility allowing us to implement virtually any admittance. They are thus particularly well suited for the present proof-of-concept study.

Although the implemented shunt admittances were chosen according to a passive control law that is in theory unconditionally stable, instabilities can occur due to sampling delays in the digital unit if they are not accounted for. This can be prevented by an appropriate discretization of the shunt transfer function to be implemented. The discretization procedure used in this work is fully described in [24].

The circuit design is based on Howland's current source [25] and similar to the one used in [15]. A description of the full DVA design realized on printed circuit boards (PCB) and used for the experimental campaign on the BluM can be found in [24].

6 EXPERIMENTAL DAMPING OF THE STRUCTURAL VIBRATIONS OF A BLUM

The experimental campaign consists of two parts: tuning the DVAs, and assessing their damping performance. In the first part, the dynamic impedance of the piezoelectric patches is directly measured with the DVAs. The patches that were used to realize the shunts in Sec. 6.1

- 6.4 correspond to Config. 3 in Fig. 5. System identification methods are used to determine the resonance frequencies and their electromechanical coupling. The tuning procedure outlined in Section 3 is then used based on these identified quantities. The sampling frequency used for the controller was about ten times the highest frequency of the first family.

To assess the performance of the proposed solution, the BluM was excited with an impact hammer on the outer side of the drum (below patch #9). The velocity was measured via a laser vibrometer at the tip of a blade located at the lower part of the drum. These signals were recorded by a Scadas Mobile data acquisition device, and postprocessed with TestLab. The time series were multiplied by an exponential window and the FRF was estimated with a standard H_1 estimator using 5 averages. The relevant measurement points for this FRF are indicated Fig. 1.

6.1 Dynamic impedances

In order to obtain the system information that is needed for a proper shunt tuning, the dynamic impedances are measured for each patch to be shunted. For this purpose, the structure was excited by a multisine signal (a periodic excitation composed of multiple sine waves with user-defined amplitude and random phase [26]). The excitation was applied consecutively, patch by patch. Fig. 10 shows the dynamic impedance as an example for patch #1 with a zoom view on some of the drum modes as well as on mode families #1 and #3. Based on numerical simulations with the same BluM model that was already used in [17], we expect the family of the first torsion modes, namely mode family #2, to be located at a normalized frequency of 2.5. However, no resonance peak appears in this frequency range in Fig. 10, indicating that there is very low coupling with this group of modes.

The dynamic impedance measurements were subject to the PolyMAX modal parameter estimation method in order to identify state-space models [27]. This method is particularly advantageous to identify modes of a mode family since the user can select modes manually in a predefined frequency range with the help of a stabilization diagram. Using curve fitting procedures with increased model order, the consistently identified modes can be considered as stabilized poles. The method provides the user with a set of selected poles and their corresponding participation factors by means of the least-squares frequency-domain (LSFD) method [28].

In Fig. 11, the Bode plot of the identified state-space model of the dynamic impedance is compared to the measurement, obtained at patch #1. The focus is on mode family #1. We observe that there is a good agreement

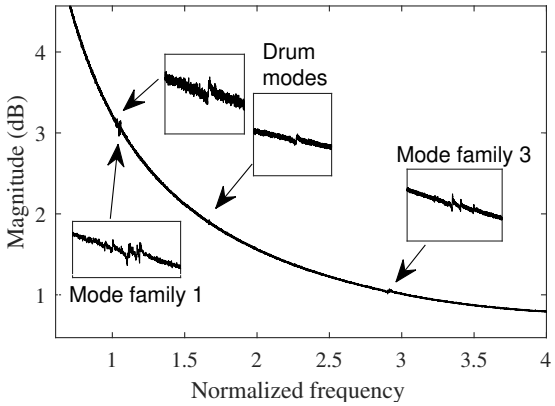

Fig. 10: Dynamic impedance of piezoelectric patch 1.

between model and measurement. In addition, considering that the BluM features 76 blades, the same amount of modes would be expected to be visible in the frequency range of a mode family. The fact that only a few resonance peaks appear in the dynamic impedance function for this patch indicates that the transducer does not feature a good electromechanical coupling with all modes of the family, hence, not all modes can be controlled with this patch. Possible reasons for this might be the mistuning that is present in the BluM, and the charge cancellation effect for modes whose characteristic wavelength is a fraction of the patch length. This fact emphasizes the importance of the simultaneous use of multiple patches in order to gain control authority over all frequencies of this mode family. Finally, the information necessary for determining the shunt parameters can be extracted from the resulting identified state-space models of the 16 piezoelectric patches. In total, a number of 19 modes could be identified in the range of the first mode family, ranging from the normalized frequencies $1.00 - 1.102$ together with three support modes at 0.602, 0.921 and 0.960.

6.2 Repeatability

By contrast with the dynamic impedance tests, the mechanical FRFs disclosed in this work can be subject to repeatability issues, since it is impossible to hit the structure with the hammer exactly at the same place every time. To check whether this is an issue here, Fig. 12 displays FRFs obtained in two subsequent tests with open-circuit patches. A good repeatability is observed for all resonances (except around a normalized frequency 1.1, but these modes are not explicitly targeted in this study). Most antiresonances feature less repeatability because they are sensitive to the excitation location. This is con-

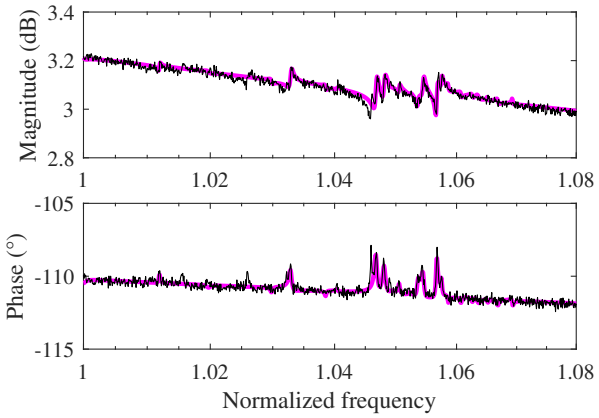

Fig. 11: Bode plot of the dynamic impedance for patch #1 (▬) and the identified model (▬).

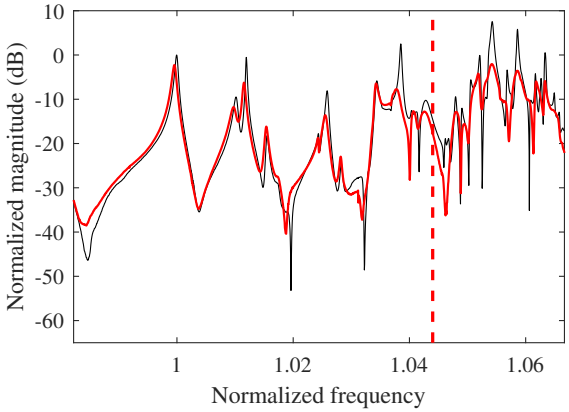

Fig. 13: Open-circuit (▬) and shunted (▬) FRF. The mean frequency is represented using (▪ ▪ ▪).

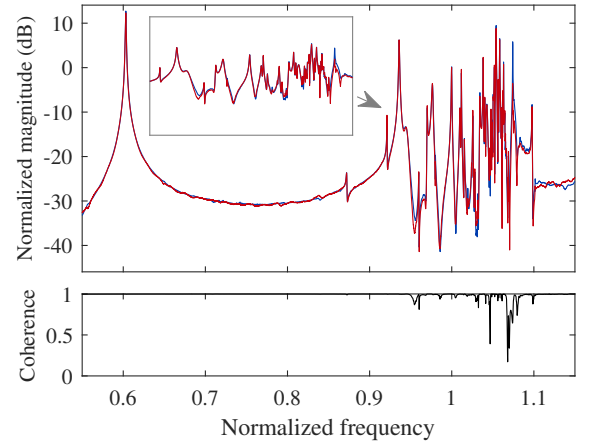

Fig. 12: Repeatability assessment: open-circuit FRFs (with a zoom on mode family #1 inset) and coherence.

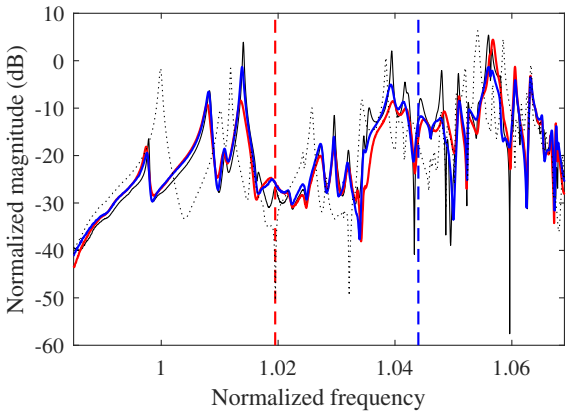

Fig. 14: Robustness study. Initial open-circuit FRF (▪ ▪ ▪), open-circuit FRF of the altered system (▬), shunts detuned (▬) and retuned (▬). The mean frequencies are represented with (▪ ▪ ▪) or (▪ ▪ ▪), respectively.

firmed by the coherence, which drops at the antiresonance frequencies due to this issue but also to the low signal-to-noise ratio in these frequency regions. Overall, repeatability issues are much smaller than the effect of the shunts, which shall now be demonstrated.

6.3 Damping performance on mode family #1

Following the mean shunt strategy, the BluM was first shunted to 16 single RL shunts targeting mode family #1. The resulting FRFs are presented in Fig. 13 comparing the uncontrolled and controlled cases. The vibrations of almost every mode of this family could be successfully attenuated, with peak amplitude reductions of up to 10dB. Naturally, it can be observed that the vibration reduction was stronger around the targeted mean frequency.

6.4 Robustness study

In a next step, the robustness of the shunts toward mistuning was investigated. To this end, 14 of the 76 small magnets fixed at the blade tips were removed randomly to alter system parameters. This resulted in changes of the resonance frequencies of up to 0.7% for mode family #1. Fig. 14 presents the open-circuit FRFs of the initial and the altered system. Frequencies and amplitudes remain normalized with respect to the first resonance frequency of mode family #1 in the initial configuration. In addition, the figure features the FRFs of the

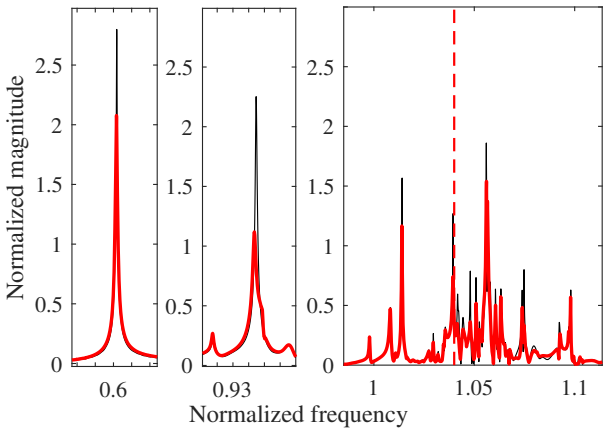

Fig. 15: FRFs of the uncontrolled system (▬) and of the system controlled by a three-stage current blocking circuit (▬). The targeted mean frequency is represented using (▬).

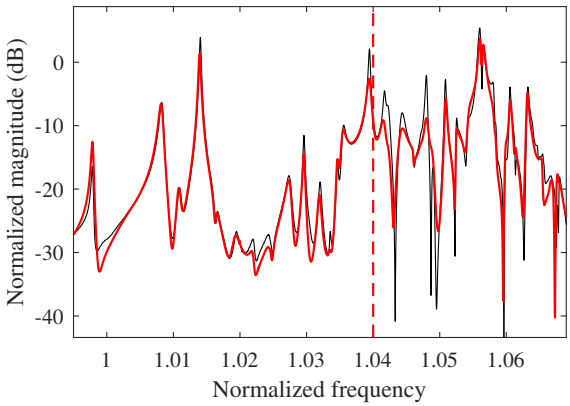

Fig. 16: FRFs in the frequency range of mode family #1 of the uncontrolled system (▬) and of the system controlled by a three-stage current blocking circuit (▬). The targeted mean frequency is represented using (▬).

altered BluM configuration controlled by detuned and retuned shunts. The former were tuned toward the initial configuration (detuned) while the latter were designed on the basis of a new system identification of the altered system (retuned).

In the detuned case, a similar damping performance (from 5 to 10dB) can be observed between 0.99 and 1.05. Yet, no or only a marginal amplitude reduction can be achieved at certain resonance peaks, e.g., at 1.008, 1.011, and 1.027. At 1.019, the shunts even cause an increase of the resonance amplitude. Around 1.044, both shunt configurations yielded large amplitude reductions since this frequency range is specifically targeted. Overall, the shunts could be retuned successfully and they offered a satisfying damping performance, even in the detuned case, as confirmed in Fig. 14. However, as for the detuned case, no significant amplitude reduction could be achieved for the resonances after 1.05. It is thus preferable to retune the shunts.

6.5 Multi-stage shunt circuits

Finally, the multi-staged shunt circuit design presented in Section 3 was realized comprising three stages tuned toward two modes of the drum support together with mode family #1. To this end, a different patch configuration (Config. 5 in Fig. 5) was used owing the fact that it featured a better coupling with multiple drum modes. The multi-staged shunt circuit was applied to the altered BluM from the previous section, with drum modes identified at the normalized frequencies 0.603 and 0.938. These two modes were targeted as isolated frequencies targeted by the two first stages, while the final stage was tuned toward the mean frequency of mode family #1 (1.040). Fig. 15 shows that the resonance amplitudes of the drum modes could be successfully attenuated (3.5 dB and 6 dB, respectively). The y-axis of this graphs is scaled in absolute values to give a better overview to the reader. In Fig. 16, the focus is set on the first mode family, presenting the amplitude values in dB for a better comparability with the results from Sections 6.3 and 6.4. It can be observed that the resonance amplitudes of almost every mode in the family could be attenuated by amounts ranging from 3 dB to 11 dB. We observe that the use of the multimodal three-stage shunt involves certain loss of control authority over the mode family. This is indicated by the fact that the attenuation of the resonance amplitudes was somewhat lower (up to 5dB) compared to the case with only one shunt.

In this experimental study, the multi-staged shunt circuit design was applied with a focus on mode family #1 and the support modes. While it can generally be used to target two mode families simultaneously as it was e.g. done in [15], this was not possible for the BluM available in the laboratory since there was no electromechanical coupling with mode family #2. Subsequent mode families are located at distinctively higher frequencies and require high sampling frequencies that cannot be straightforwardly achieved using the available hardware which represents a limiting factor for this experimental campaign. However, given the results presented in Fig. 15 and 16, we can state that a proof of concept could successfully be demonstrated.

7 DISCUSSION

Following this work comes a series of questions about a concrete realization. The first one concerns the adequacy of the proposed approach for more realistic situations, such as the response to aerodynamic engine-order excitations. Since the present work demonstrated the increased modal damping brought by the DVAs and since this property is independent on the considered input/output pair (as long as the system remains linear), good performance is also expected for this kind of loads. Further fine-tuning may however be required if some of the problematic modes do not feature a satisfying electromechanical coupling.

Next comes the question of how these DVAs could be integrated in such a structure. A MicroLabBox was used for convenience in this work, requiring bulky cables and connectors. Using much smaller microprocessors, as well as miniaturized electronics will favor the integration. Wiring should be simplified due to the decentralized approach of the proposed control solution, but should also be performed carefully to withstand the rotation loads.

The two main downsides of DVAs are their need for a power supply and the possibility of instabilities. Regarding the former, a sufficient amount of energy could be harvested from the rotation. This harvesting system and the electronic elements used in the DVAs should carefully be designed to accommodate for the high voltages generally featured by piezoelectric transducers. As for the latter, a sufficiently high sampling frequency needs to be chosen (typically at least 10 times the frequency of interest) and a proper discretization procedure needs to be used.

The general limits of piezoelectric shunts for this application should now be discussed. First, because of the position and distribution of the piezoelectric patches, some modes may not be damped enough. This could be improved by using a larger number of smaller patches, at the expense of more required shunts. Alternatively, a more thorough optimization of the patches size and shape could be performed. Second, piezoelectric materials have a temperature limit (usually equal to half the Curie temperature of the material). While this may not be an issue if appropriate materials are selected for the cold parts of the engine, such as the fan and low-pressure compressor, this approach cannot be used in the high-temperature parts.

8 CONCLUSIONS AND OUTLOOK

Moving from a bladed rail [15] to a complex industrial structure, the BluM, the strategy presented in Section 3 was successfully validated experimentally. More specifically, the resonant vibrations of mode family #1 together with two drum modes could be mitigated thanks to a multi-staged shunt design. In contrast to the analog shunts used in [10, 13, 29], a digital implementation of the shunts offers great advantages such as a rapid and easy retuning and a compact realization on PCBs.

The proof of concept presented in this work paves the way for more robust industrial implementations. Further research could progress toward a self-optimization of the DVAs, e.g. by automating the system identification of the plant transfer functions. Moreover, a thorough study of the effects of different measurement locations and excitation types on shunt performance could be of interest, e.g. with an engine-order excitation approaching the operating conditions of the BluM. Lastly, a rotating BluM could also be considered, in which the energy generated from the rotational energy could be used to power the DVAs.

ACKNOWLEDGEMENTS

This work was supported by the Fonds de la Recherche Scientifique - FNRS under Grant n° FRS-FNRS PDR T.0124.21, and the SPW under WALInnov Grant n° 1610122, which are gratefully acknowledged. Ghislain Raze is a Postdoctoral Researcher of the Fonds de la Recherche Scientifique - FNRS.

REFERENCES

[1] Tacher, A., 2022, "Forced response and stability of mistuned structures subject to the coriolis effect," Doctoral thesis, Ecole centrale de Lyon.

[2] Charleux, D., Gibert, C., Thouverez, F., and Dupeux, J., 2006, "Numerical and Experimental Study of Friction Damping Blade Attachments of Rotating Bladed Disks," *International Journal of Rotating Machinery,* **2006**, July, p. e71302 Publisher: Hindawi.

[3] Petrov, E. P., and Ewins, D. J., 2006, "Advanced Modeling of Underplatform Friction Dampers for Analysis of Bladed Disk Vibration," *Journal of Turbomachinery,* **129**(1), Feb., pp. 143–150.

[4] Laxalde, D., Gibert, C., and Thouverez, F., 2009, "Experimental and Numerical Investigations of Friction Rings Damping of Blisks," In Turbo expo: power for land, sea, and air, American Society of Mechanical Engineers Digital Collection, pp. 469–479.

[5] Nguyen, N., 2000, Blading system and method for controlling structural vibrations, Aug.

[6] Yu, H., and Wang, K. W., 2007, "Piezoelectric Networks for Vibration Suppression of Mistuned Bladed Disks," *Journal of Vibration and Acoustics,* **129**(5), May, pp. 559–566.

[7] Kauffman, J. L., and Lesieutre, G. A., 2012, "Piezoelectric-Based Vibration Reduction of Turbomachinery Bladed Disks via Resonance Frequency Detuning," *AIAA Journal,* **50**(5), May, pp. 1137–1144.

[8] Thierry, O., De Smet, O., and Deü, J., 2016, "Vibration reduction of a woven composite fan blade by piezoelectric shunted devices," *Journal of Physics: Conference Series,* **744**, Sept., p. 012164.

[9] Mokrani, B., 2015, "Piezoelectric Shunt Damping of Rotationally Periodic Structures," Doctoral thesis, Université Libre de Bruxelles, Brussels, Belgium.

[10] Mokrani, B., Bastaits, R., Horodinca, M., Romanescu, I., Burda, I., Vigiué, R., and Preumont, A., 2014, "Passive piezo damping of rotationally periodic structures with application to a bladed drum," In Proceedings of ISMA 2014 including USD 2014.

[11] Zhou, B., Thouverez, F., and Lenoir, D., 2014, "Vibration Reduction of Mistuned Bladed Disks by Passive Piezoelectric Shunt Damping Techniques," *AIAA Journal,* **52**(6), pp. 1194–1206 Publisher: American Institute of Aeronautics and Astronautics _eprint: https://doi.org/10.2514/1.J052202.

[12] Viguié, R., Verhelst, D., Preumont, A., and Mokrani, B., 2015, Piezoelectric damper system for an axial turbomachine rotor (US Patent US10125794B2) Assignee: Safran Aero Boosters SA, Université Libre de Bruxelles ULB.

[13] Mokrani, B., Bastaits, R., Horodinca, M., Romanescu, I., Burda, I., Viguié, R., and Preumont, A., 2015, "Parallel Piezoelectric Shunt Damping of Rotationally Periodic Structures," *Advances in Materials Science and Engineering,* **2015**, pp. 1–12.

[14] Paknejad, A., Jamshidi, R., Pathak, S., and Collette, C., 2023, "Active Vibration Mitigation of Bladed Structures With Piezoelectric Patches by Decentralized Positive Position Feedback Controller," *Journal of Engineering for Gas Turbines and Power,* **145**(2), Feb., p. 021003.

[15] Dietrich, J., Raze, G., and Kerschen, G., 2022, "Multimodal shunt damping of mechanical structures using multiple digital vibration absorbers," *Engineering Research Express,* **4**(4), Dec., p. 045028.

[16] Fleming, A. J., Behrens, S., and Moheimani, S. O. R., 2000, "Synthetic impedance for implementation of piezoelectric shunt-damping circuits," *Electronics Letters,* **36**(18), p. 1525.

[17] Raze, G., 2021, "Piezoelectric Digital Vibration Absorbers for Multimodal Vibration Mitigation of Complex Mechanical Structures," Doctoral Thesis, Université de Liège, Liège, Apr.

[18] Saravanamuttoo, H. I. H., Rogers, G. F. C., and Cohen, H., 2001, *Gas Turbine Theory* Pearson Education.

[19] Wu, S.-Y., 1998, "Method for multiple-mode shunt damping of structural vibration using a single PZT transducer," In Proceedings Volume 3327, Smart structures and materials 1998: passive damping and isolation, pp. 159–168.

[20] Agneni, A., Del Sorbo, M., Mastroddi, F., and Pollo, G. M., 2006, "Multi-modal damping by shunted piezo-patches: Possible aeroelastic applications," *International Journal of Applied Electromagnetics and Mechanics 24*.

[21] Raze, G., Paknejad, A., Zhao, G., Collette, C., and Kerschen, G., 2020, "Multimodal vibration damping using a simplified current blocking shunt circuit," *Journal of Intelligent Material Systems and Structures,* **31**(14), pp. 1731–1747.

[22] Raze, G., Dietrich, J., and Kerschen, G., 2022, "Tuning and performance comparison of multiresonant piezoelectric shunts," *Journal of Intelligent Material Systems and Structures,* **33**(19), pp. 2470–2491.

[23] Piefort, V., 2001, "Finite Element Modelling of Piezoelectric Active Structures," PhD thesis, Université Libre de Bruxelles.

[24] Dietrich, J., 2023, "Piezoelectric digital vibration absorbers for vibration mitigation of bladed structures," Doctoral Thesis, University of Liege, Liège, Belgium, Aug.

[25] Horowitz, P., and Hill, W., 2015, *The Art of Electronics*, 3. ed. Cambridge University Press.

[26] Schoukens, J., Vaes, M., and Pintelon, R., 2016, "Linear System Identification in a Nonlinear Setting: Nonparametric Analysis of the Nonlinear Distortions and Their Impact on the Best Linear Approximation," *IEEE Control Systems,* **36**(3), June, pp. 38–69.

[27] Peeters, B., Van der Auweraer, H., Guillaume, P., and Leuridan, J., 2004, "The PolyMAX Frequency-Domain Method: A New Standard for Modal Parameter Estimation?," *Shock and Vibration,* **11**(3-4), pp. 395–409.

[28] Heylen, W., Lammens, S., and Sas, P., 2007, *Modal analysis theory and testing*, 2. ed. Katholieke Univ. Leuven, Departement Werktuigkunde, Leuven.

[29] Mokrani, B., Bastaits, R., Viguié, R., and Preumont, A., 2012, "Vibration damping of turbomachinery components with piezoelectric transducers: Theory and Experiment," In PROCEEDINGS OF ISMA2012-USD2012.